

A dynamic actuation model for magnetostrictive materials

N N Sarawate and M J Dapino

Department of Mechanical Engineering, The Ohio State University, Columbus, OH 43210, USA

E-mail: sarawate.1@osu.edu and dapino.1@osu.edu

Received 7 May 2008, in final form 5 September 2008

Published 10 October 2008

Online at stacks.iop.org/SMS/17/065013

Abstract

We quantify the dependence of strain on dynamic magnetic field in magnetostrictive transducers. Dynamic eddy current losses are modeled as a one-dimensional (1D) magnetic diffusion problem in cylindrical coordinates. The constitutive magnetostrictive response to an average diffused magnetic field is quantified with the Jiles–Atherton model. The transducer is represented as a lumped-parameter, single-degree-of-freedom resonator with force input dictated by the magnetostriction. This equivalent force is expressed as a summation of Fourier series terms. The total dynamic strain output is obtained by superposition of strain solutions due to each harmonic of the force input.

(Some figures in this article are in colour only in the electronic version)

Magnetostrictive materials deform when exposed to magnetic fields and change their magnetization state when stressed. These responses are nonlinear, hysteretic, and frequency-dependent. Several models exist for describing the dependence of strain on field at quasi-static frequencies. The strain vs field response changes significantly relative to the quasi-static case as the frequency of applied field is increased. Modeling the dynamic strain vs field hysteresis relationship has been a challenging problem because of the inherent nonlinear and hysteretic behavior of magnetostrictive materials and complexity of dynamic magnetic losses and structural vibrations of magnetostrictive transducers. Previous attempts have involved mathematical techniques such as the Preisach model [1–3] and genetic algorithms [4]. A phenomenological approach including eddy currents and structural dynamics was recently presented [5].

The chief intent of this paper is to present a new approach for modeling the strain vs field hysteresis relationship of magnetostrictive materials driven with dynamic magnetic fields in actuator devices (figure 1). The approach builds on our prior models for dynamic hysteresis in ferromagnetic shape memory Ni–Mn–Ga [6].

Application of an alternating magnetic field to a conducting material such as Terfenol-D results in the generation of eddy currents and an internal magnetic field which partially offsets the applied field. The relationship between the eddy currents and applied fields is described

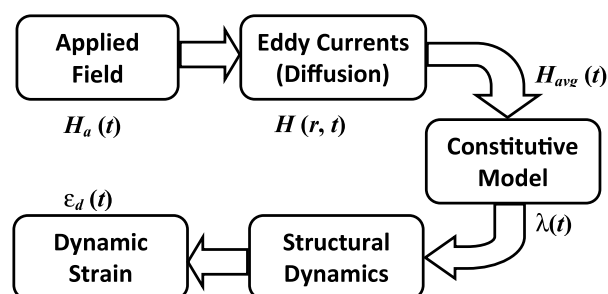


Figure 1. Flow chart representing a dynamic model for magnetostrictive actuators.

by Maxwell's electromagnetic equations. Assuming that the magnetization is uniform and does not saturate, the diffusion equation describing the magnetic field inside a 1D conducting medium of cylindrical geometry has the form [7]

$$\frac{\partial^2 H}{\partial r^2} + \frac{1}{r} \frac{\partial H}{\partial r} = \mu \bar{\sigma} \frac{\partial H}{\partial t}, \quad (1)$$

where $\bar{\sigma}$ is electrical conductivity and μ is magnetic permeability.

For harmonic applied fields, the boundary condition at the edge of the cylindrical rod ($r = R$) is given by,

$$H(R, t) = H_0 e^{i\omega t}, \quad (2)$$

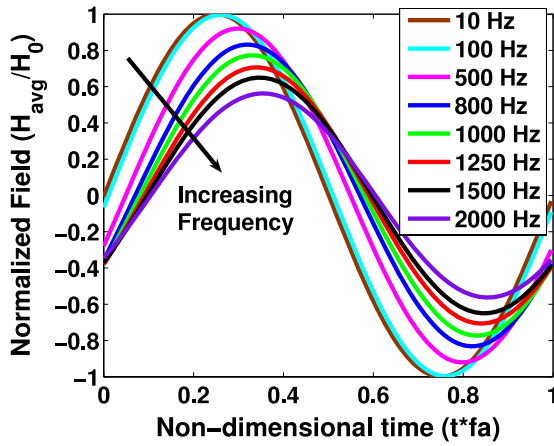


Figure 2. Normalized average field vs non-dimensional time.

where H_0 is the amplitude and $\omega = 2\pi f_a$ is the circular frequency (rad s^{-1}) of the magnetic field on the surface of the magnetostrictive material. The solution to (1) gives the magnetic field values $H(r, t)$ at radius r and time t . To estimate the effective field, we average the magnetic field by integrating over the cross-section of the material. Figure 2 shows the average field waveforms at several applied field frequencies. With increasing frequency, the magnetic field diffusion results in a decrease in the amplitude and an increase in the phase lag of the averaged field relative to the field on the surface of the material.

It is proposed that the material response is dictated by this averaged field. The constitutive material response is obtained from the Jiles–Atherton model [8] in combination with a quadratic model for the magnetostriction. It is assumed that the relationship between magnetostriction and field does not include additional dynamic effects. The process to obtain the magnetostriction has been detailed before [8]. The magnetostriction is assumed to be dependent on the square of magnetization as

$$\lambda = \frac{3}{2} \left(\frac{M}{M_s} \right)^2, \quad (3)$$

with λ magnetostriction, M magnetization, and M_s saturation magnetization. The quadratic relationship is justified by the use of a sufficiently large bias stress in the magnetostrictive material [9]. At low magnetic fields, the total strain (ε) is given by the superposition of the magnetostriction and elastic strain,

$$\varepsilon = \lambda + \sigma/E, \quad (4)$$

in which E is the open-circuit elastic modulus. Note that equation (4) gives the material response to a dynamic average field. However, the response of a dynamic actuator including a magnetostrictive driver and external load must be obtained by incorporating structural dynamics.

A dynamic model of a magnetostrictive actuator is illustrated in figure 3. The actuator is modeled as a single-degree-of-freedom lumped-parameter resonator in which a magnetostrictive rod acts as an equivalent spring of stiffness EA/L , with A the area and L the length. This equivalent spring is in parallel with the load stiffness k , which is also

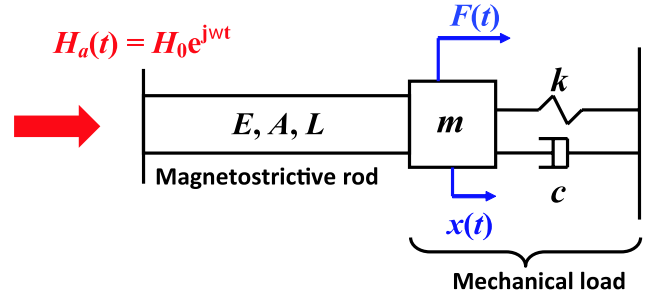


Figure 3. Dynamic model of a typical magnetostrictive actuator.

used to pre-compress the rod. The overall system damping is represented by lumped damping coefficient c ; the combined mass of the magnetostrictive rod and output pushrod are modeled as a lumped mass m . When an external field $H_a(t)$ is applied to the rod, an equivalent force $F(t)$ is generated which drives the motion of the mass.

The dynamic system equation is written as

$$m\ddot{x} + c\dot{x} + kx = F(t) = -\sigma(t)A, \quad (5)$$

with x the displacement of mass m . Substitution of (4) into (5) combined with $\varepsilon = x/L$ gives

$$m\ddot{x} + c\dot{x} + \left(k + \frac{AE}{L} \right) x = AE\lambda(t). \quad (6)$$

Equation (6) represents a second-order dynamic system driven by the magnetostriction. The dependence of magnetostriction on applied field is nonlinear and hysteretic, and follows the dynamics of a zero-order system, i.e. the magnetostriction does not depend on the frequency of the applied magnetic field. For periodic applied fields, the magnetostriction also follows a periodic waveform and hence the properties of Fourier series are utilized to express the magnetostriction as

$$\lambda(t) = \sum_{n=0}^N |\Lambda_n| \cos(2\pi n f_a t + \angle \Lambda_n), \quad (7)$$

where $|\Lambda_n|$ and $\angle \Lambda_n$ respectively represent the magnitude and phase of the n th harmonic of actuation frequency f_a . The term $AE\lambda(t)$ represents an equivalent force that dictates the dynamic response of the actuator. Using the superposition principle, the total dynamic strain (ε_d) is given by

$$\begin{aligned} \varepsilon_d(t) = \frac{x(t)}{L} = \frac{EA}{EA + kL} \sum_{n=0}^N |\Lambda_n| [1 - (nf_a/f_n)^2]^{-2} \\ + (2\zeta nf_a/f_n)^{-1/2} \cos \left[2\pi n f_a t + \angle \Lambda_n \right. \\ \left. - \tan^{-1} \left(\frac{2\zeta nf_a/f_n}{1 - (nf_a/f_n)^2} \right) \right], \end{aligned} \quad (8)$$

with f_n natural frequency and ζ damping ratio.

Figure 4 shows a comparison of model results and experimental measurements collected from a Terfenol-D transducer [10]. The model parameters, which remain the same at all the frequencies, are: $\mu = 5\mu_0$, $1/\bar{\sigma} = 58e - 8 \Omega\text{m}$,

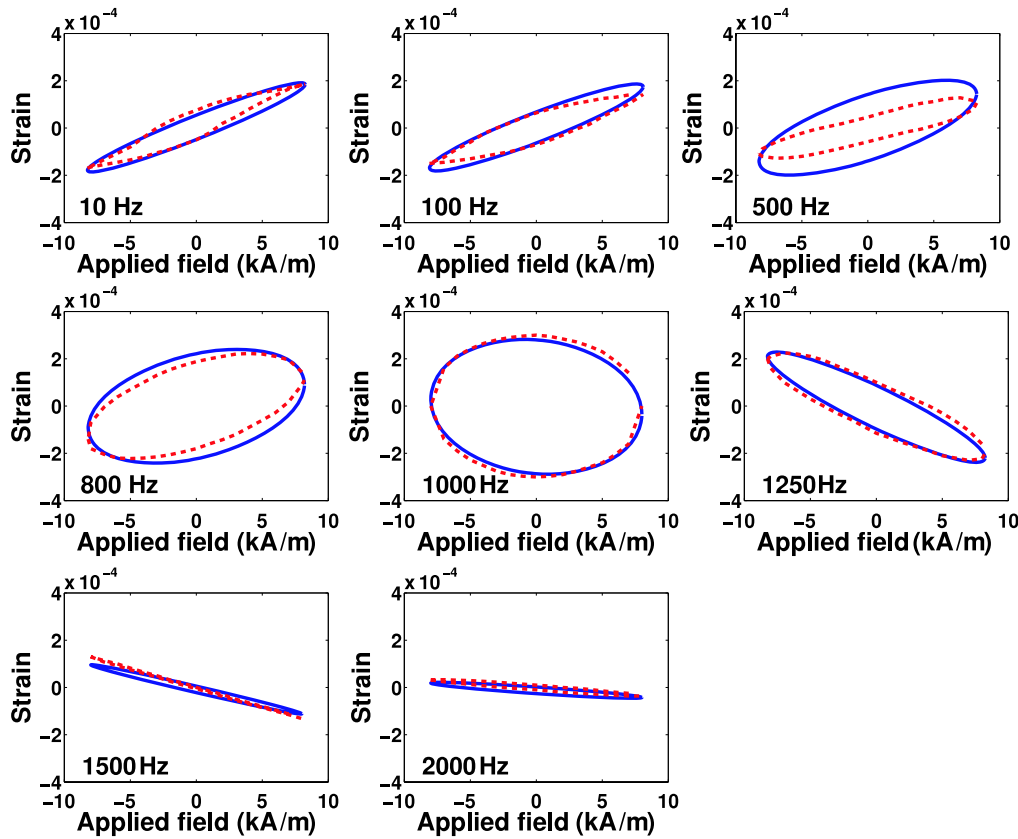


Figure 4. Strain vs applied field at varied actuation frequencies. Dashed line: experimental, solid line: model.

$f_n = 1150$ Hz, and $\zeta = 0.2$. The model accurately describes the changing hysteresis loop shape and peak-to-peak strain magnitude with increasing frequency. These results show improvement over previous work using the same data [5]. With increasing frequency, the strain lags behind the applied field due to the combined contributions of the system vibrations and dynamic magnetic losses.

The maximum strain and largest hysteresis loop area are seen at a frequency near resonance (1000 Hz), indicating a phase angle of about -90° . As the frequency increases beyond resonance, the strain magnitude diminishes rapidly accompanied by further delay of the phase angle.

Model results and experimental data are shown in the non-dimensional frequency domain or harmonic order domain in figure 5. It is noted that the frequency spectra contain the contribution of higher harmonics of the actuation frequency because of the nonlinear nature of the system. However, Terfenol-D exhibits relatively small hysteresis compared to ferromagnetic shape memory alloys such as Ni-Mn-Ga. Therefore, the contribution of higher harmonics of the actuation frequency is not as significant as seen in Ni-Mn-Ga [6]. In figure 6, we plot the variation of the magnitude and phase of the first harmonic. Note that the frequency at which the peak strain magnitude is observed (1000 Hz) occurs below the mechanical resonance frequency (1150 Hz). This is because the contribution of actuator dynamics to the phase angle is complemented by the phase angle due to magnetic field diffusion. Thus, the phase angle of -90° and hence

the corresponding maximum strain magnitude occur below mechanical resonance.

A model is presented to describe the dependence of strain on applied fields in magnetostrictive actuators operated dynamically. The essential components of the model include the magnetomechanical constitutive response (obtained through the Jiles-Atherton model), magnetic field diffusion, and actuator dynamics. Our intuitive and physics-based approach has been successfully implemented for two classes of magnetically activated smart materials: Terfenol-D and Ni-Mn-Ga [6]. The presented method can be extended to arrive at the input field profile which will result in a desired strain profile at a given frequency. If the direction of flow in figure 1 is reversed, the input field profile can be designed from a desired strain profile. It is comparatively easy to obtain the inverse Fourier transform, whereas calculation of the average field from a desired strain profile through a constitutive model, and estimation of the external field from the averaged diffused field inside the material can be complex.

The frequency spectra of the strain include even and odd harmonics. The contribution of higher harmonics is very small because the Terfenol-D actuator under consideration is biased with a field of 16 kA m^{-1} , which results in reduced hysteresis. An unbiased actuator exhibits larger hysteresis and would consist of only even harmonics, with increased contribution of the higher harmonics. The biased actuator resonates when the applied field frequency is close to the natural frequency of the actuator, whereas an unbiased actuator resonates when

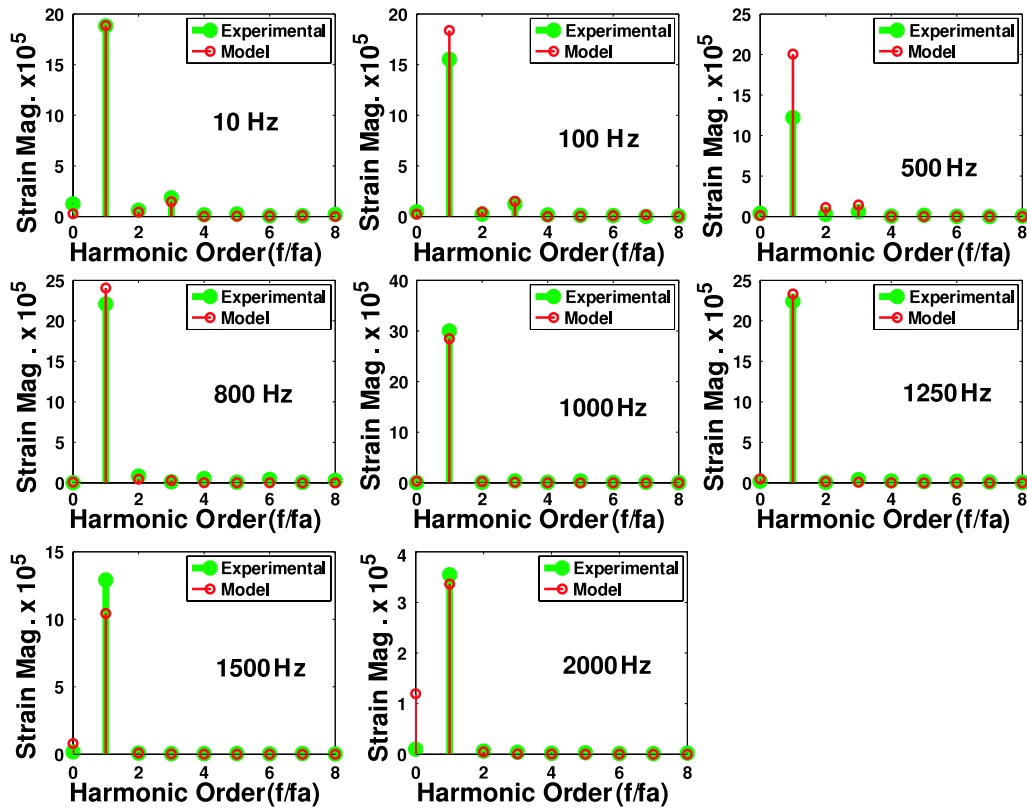


Figure 5. Frequency domain strain magnitudes at varied actuation frequencies. Dashed line: experimental, solid line: model.

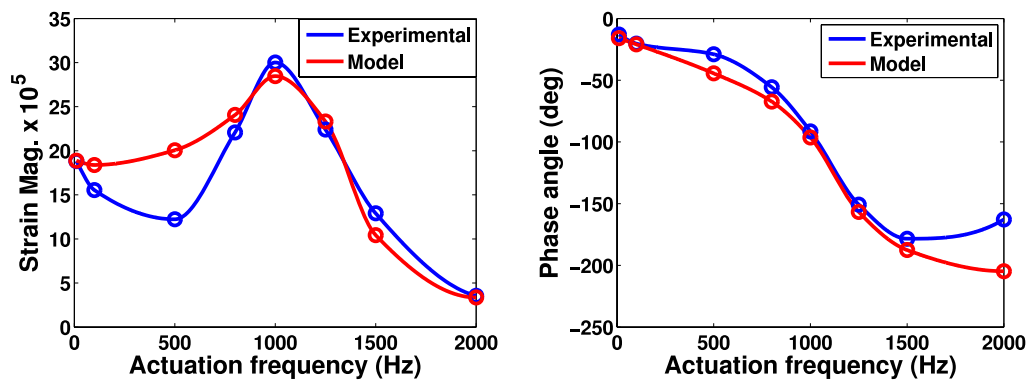


Figure 6. Variation of magnitude and phase of the first harmonic.

the applied field frequency is half of the natural frequency. Our approach can successfully model the unbiased actuator configuration as well [6].

Acknowledgments

This work was supported in part by the National Science Foundation under Grant CMS-0409512, Dr Shih-Chi Liu, Program Director. We are grateful to the member organizations of the Smart Vehicle Concepts Center (www.SmartVehicleCenter.org) and the National Science Foundation Industry/University Cooperative Research Centers program (www.nsf.gov/eng/iip/lucrc) for providing financial support. Additional support for NS was provided by the Smart Vehicle Concepts Center Fellowship Program.

References

- [1] Tan X and Baras J S 2004 *Automatica* **40** 1469
- [2] Davino D, Natale C, Pirzori S and Visone C 2004 *Physica B* **343** 112
- [3] Bottauscio O, Chiampi M, Lovisolo A, Roccato P E and Zucca M 2008 *J. Appl. Phys.* **103** 07F121
- [4] Cao S, Wang B, Zheng J, Huang W, Sun Y and Xiang Q 2006 *IEEE Trans. Magn.* **42** 911
- [5] Huang W, Wang B, Cao S, Sun Y, Weng L and Chen H 2007 *IEEE Trans. Magn.* **43** 1381
- [6] Sarawate N and Dapino M 2008 *IEEE Trans. Magn.* **44** 566
- [7] Knoepfel H 2000 *Magnetic Fields: A Comprehensive Theoretical Treatise for Practical Use* (New York: Wiley)
- [8] Jiles D C 1995 *J. Appl. Phys.* **28** 1537
- [9] Dapino M J, Smith R C, Faidley L E and Flatau A B 2000 *J. Intell. Mater. Syst. Struct.* **11** 135
- [10] Calkins F T 1997 *PhD Thesis* Iowa State University